©Freund Publishing House Ltd. London International Journal of Turbo and Jet Engines, 18, 47-58(2001)

Simultaneous Prediction of External Flow-Field and Temperature in Internally Cooled 3-D turbine Blade Material

Zhen-Xue Han[1]
Multidisciplinary Analysis, Inverse Design, and Optimization (MAIDO) Program
Department of Mechanical and Aerospace Engineering, UTA Box 19018
The University of Texas at Arlington, Arlington, TX 76019, USA. han@mae.uta.edu

Brian H. Dennis[2]
Department of Aerospace Engineering, 233 Hammond Building
The Pennsylvania State University, University Park, PA 16802, U.S.A. bhd102@psu.edu

George S. Dulikravich[3,*]
Multidisciplinary Analysis, Inverse Design, and Optimization (MAIDO) Program
Department of Mechanical and Aerospace Engineering, UTA Box 19018
The University of Texas at Arlington, Arlington, TX 76019, USA. gsd@mae.uta.edu

Abstract

A two-dimensional (2-D) and a three-dimensional (3-D) conjugate heat transfer (convection-conduction) prediction codes were developed where the compressible turbulent flow Navier-Stokes equations are solved simultaneously in the flow-field and in the solid material of the structure, thus automatically predicting correct magnitudes and distribution of surface temperatures and heat fluxes. The only thermal boundary conditions are the convection heat transfer coefficients specified on the surfaces of the internal coolant flow passages and the coolant bulk temperature of internally cooled gas turbine blade. This approach eliminates the need to specify hot surface temperature or heat flux distribution. The conjugate codes use hybrid unstructured triangular/quadrilateral grids in 2-D and unstructured prismatic grids in 3-D throughout the flow-field and in the surrounding structure. The codes are capable of conjugate heat transfer prediction in arbitrarily shaped internally cooled configurations. The computer codes have been successfully tested on internally cooled turbine airfoil cascades and 3-D turbine blades by the conjugate solution of the flow field and the temperature field inside the structure.

Key words: conjugate heat transfer, numerical methods, turbomachinery, axial turbines

Introduction

During thermal analysis of any structure exposed to a moving fluid of a different temperature, it is essential to specify thermal boundary conditions (temperature, heat flux, or a combination of these) on the solid surface in contact with the moving fluid. In the case of internally cooled gas turbine blades, this task still requires a large degree of experience on the part of the thermal analyst. Such thermal boundary conditions are specified on both the "hot" outside surface of the blade (so that the hot gas flow-

[1] Visiting Research Associate
[2] Graduate Research Assistant
[3] Professor and Director of MAIDO Laboratory
[*] All correspondence should be addressed to Prof. G.S. Dulikravich

field governing equations could be integrated) and on the "cold" surfaces of the coolant passages inside the blade. By specifying all thermal boundary conditions we are forcing both the hot gas flow-field and the coolant flow-field to perform the tasks that they physically might not be able to achieve with the given geometry of the blade and the global flow-field parameters. Thus, this is an inconsistent procedure. The problem is usually remedied by a tedious and costly iteration that involves sequentially performing numerical predictions of the temperature field in the moving hot gas and temperature field inside the blade material.

A less risky procedure is the sequential conjugate heat transfer analysis (Martin *et al.*, 1999). That is, a numerical prediction procedure that iteratively combines two analysis codes: the prediction of the entire hot gas flow-field, and a prediction of the heat conduction inside the blade material. This approach can be unstable since both temperatures and heat fluxes on a solid surface exposed to the moving fluid will have to be updated iteratively by both codes each of which can use different methods, have significantly different convergence properties, and provide different numerical accuracies.

The full conjugate (concurrent) analysis is where a single computational fluid dynamics (CFD) analysis code is used to integrate the conservation laws simultaneously in the entire domain comprised of both the hot gas flow-field and the solid blade material. The only changes needed in the CFD code are that in the solid blade material it should: a) not solve mass and momentum balance equations, b) explicitly use zero velocities, c) use solid blade material specific heat coefficient and thermal conductivity coefficient. Such a fully conjugate code therefore requires thermal boundary conditions to be prescribed on the coolant passage walls only. Thus, this type of the conjugate heat transfer analysis automatically predicts the correct hot surface temperature and heat flux distributions that are compatible with the predicted hot gas flow-field.

Pelletier *et al.* (1995) numerically studied the hydrodynamic and thermal conjugated heat transfer of forced convection around cylinders in a channel and free convection around a pin-fin. An adaptive finite element was used. The numerical results agreed well with the experimental data. Recently, Heidmann *et al.* (1999) numerically simulated the three-dimensional coupled internal/external flow-fields of a realistic film-cooled turbine vane. However, the blade wall was treated as an isothermal surface. This was remedied by a code named CHT-Flow which is a conjugate fluid flow and heat transfer solver developed by Bohn *et al.* (1999). They studied a convectively cooled axial turbine blade with a ribbed serpentine-shaped cooling passage and cooling gas ejection at the blade tip and the trailing edge. Both NASA code (Heidmann *et al.*, 1999) and CHT-Flow code use multi-block structured grids. Due to the complex geometry of the ribbed coolant flow passages, the multi-block grid generation in the coolant flow regions and the solid material regions of a realistic hot gas turbine require significant time to generate.

This paper presents the numerical results of 2-D and 3-D fluid flow and heat transfer conjugate simulations that utilize hybrid structured/unstructured grids. The main advantage of this formulation is a higher degree of flexibility in treating realistic geometric configurations. In addition, the generation of non-structured grids and especially the hybrid prismatic grids requires less time than the block-structured grid generation for complex realistic internally cooled turbine blades. These are important aspects of any future attempts to use conjugate analysis codes in optimization of 3-D cooled blade shapes.

Numerical Procedure

The integral form of Favre averaged Navier-Stokes equations and k-ω turbulence model equations with transition model (Chima, 1994; Larsson, 1997) were solved numerically. The spatial domain was divided into a finite number of triangles and/or quadrilaterals 92-D) or tetrahedrons and/or hexahedrons and/or prisms and/or pyramids (3-D). The governing equations were discretized by finite

volume method and integrated in time using an explicit multi-stage Runge-Kutta scheme with local time stepping. The vertex-centered scheme was used. In this scheme the volume-averaged state variables were solved at each grid node – the centroid of each 'dual mesh' which serves as a control volume. To accelerate the convergence to steady state solution, local time-stepping and pseudo-Laplacian residual smoothing techniques were used (Jameson and Mavriplis, 1986). A pre-conditioning method (Weiss and Smith, 1995) was used to accelerate the convergence to a steady state in the low-Mach-number domains of the flow-field.

The finite volume approach requires computation of the fluxes across each cell face. The convective fluxes were computed using the Roe flux-difference splitting approach (Roe, 1986) with upwind-biased interpolations. The central difference scheme was used to calculate the viscous terms in the governing equations. The Cartesian derivatives were calculated in the stencil presented by Frink (1994) and Mitchell (1994) or using the least-squares approach. In this work, the flow-field governing equations and the turbulence model equations were solved separately at each Runge-Kutta stage.

Boundary Conditions

Four different types of flow-field boundary conditions were involved with this numerical simulation: the inlet boundary, the outlet boundary, the solid wall boundary, and the periodic boundary. All the boundary conditions were implemented with a half-boundary cell stencil. At the inlet and outlet boundaries, one-dimensional Riemann invariants were used to specify the incoming and outgoing boundary conditions. At the periodic boundaries, the flow-field variables were duplicated for the periodic cell pairs or vertex pairs. At the solid walls, a no-slip boundary condition was imposed for velocity, and pressure was extrapolated from the nearest flow-field grid point. The density on the wall was calculated from the thermal boundary condition and the equation of state.

When the flow-field around the blade and the heat conduction inside the blade material are solved simultaneously, there is a heat transfer across the solid wall. Continuities of temperature and heat flux must be enforced at this fluid/solid interface. That is,

$$T_{fluid} = T_{solid} \tag{1}$$

$$\kappa_{fluid} \left.\frac{\partial T}{\partial n}\right|_{fluid} = \kappa_{solid} \left.\frac{\partial T}{\partial n}\right|_{solid} \tag{2}$$

From these equalities, we can see that $\left.\frac{\partial T}{\partial n}\right|_{fluid}$ is not equal to $\left.\frac{\partial T}{\partial n}\right|_{solid}$ because κ_{fluid} is different from κ_{solid}. In other words, temperature is continuous, but normal temperature derivative is discontinuous across the fluid/solid interface. During the numerical procedure, specifying the temperature boundary condition of the flow field with the wall temperature calculated from the solid side satisfies the temperature continuity. Specifying the heat flux boundary condition of the solid temperature field with the value calculated from the flow-field side satisfies the heat flux continuity condition. In this way, equation (2) is iteratively enforced at the fluid/solid interface during flow-field and heat conduction conjugate calculations.

Two-Dimensional Validation

To demonstrate the numerical methods mentioned above for the combined flow-field/heat conduction problems, several cases were studied. Firstly, the 2-D code was validated for a transonic turbine airfoil cascade flow against the experimental data provided by Giel *et al.* (1998; 1999). This was to test the capability and accuracy of the code to predict the complex transonic turbulent flow-fields. The airfoil wall was assumed to be adiabatic. The 2-D hybrid unstructured grid consisted of eleven structured clustered O-grid layers (quadrilaterals)

around the airfoil with the rest of the flow-field discretized with triangles (Fig. 1). The predicted pressure (non-dimensionalized by the inlet total pressure) distribution along the airfoil contour was compared with the experimental data (Fig. 2) showing good agreement.

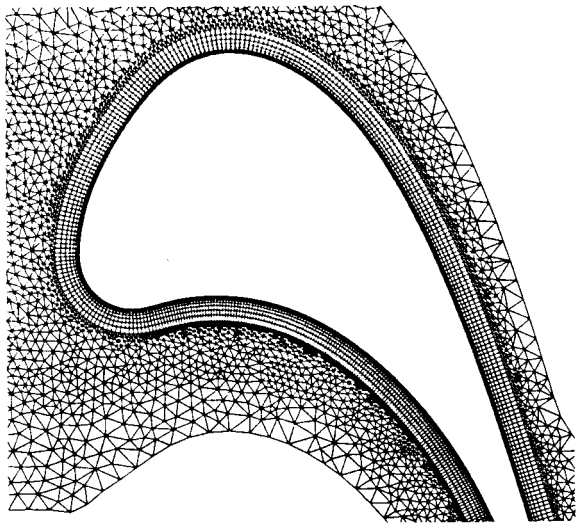

Fig. 1: Hybrid unstructured grid (leading edge region).

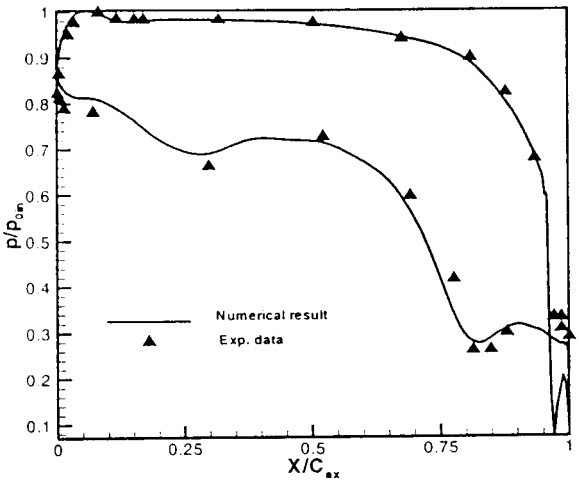

Fig. 2: Nondimensionalized pressure on the blade surface [experimental data provided by P. Giel (1999)].

The CFD code was also validated against aero-thermal data for a highly loaded VKI transonic turbine guide vane with isothermal walls (Arts *et al.* 1990). Experimental data are available for this cascade at different flow conditions including incoming free stream turbulence intensity. The test case MUR222 was chosen to test the ability of our code to simulate the transonic flows with high free stream turbulence intensity and heat transfer across the wall. The inlet total pressure was 0.822 bar, inlet total temperature was 409.2 K, inlet turbulence intensity was 6%, and the exit average pressure was 0.369 bar. Figure 3 shows the computational grids

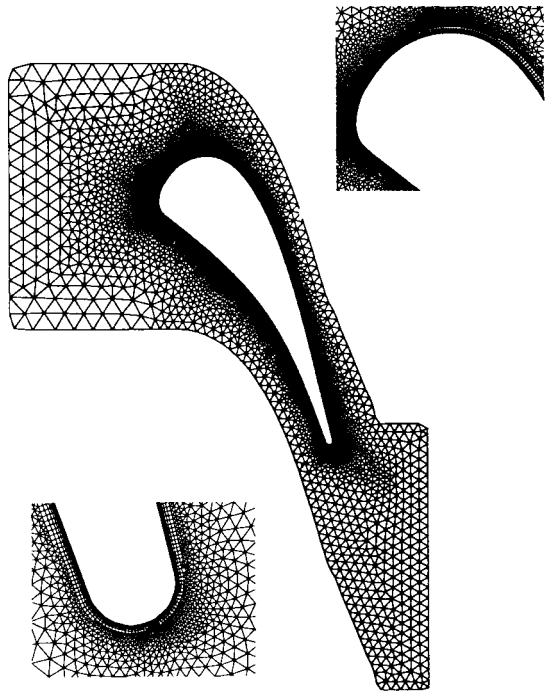

Fig. 3: Hybrid grids for CFD computations.

with enlarged leading edge and trailing edge regions. The first O-grid line distance from the blade surface was 10^{-6} m. There were 12376 grid points, 11718 triangles and 18363 quadrilaterals. The computed Mach number contours are shown in Fig. 4. The computed inlet Mach number was 0.15. These were the same values as in the experimental results. The computed exit Mach number was also around the experimental level of 1.135. The trailing edge shock wave was observed from both Mach number contours and temperature contours (Fig. 5). A comparison of computed convective heat transfer

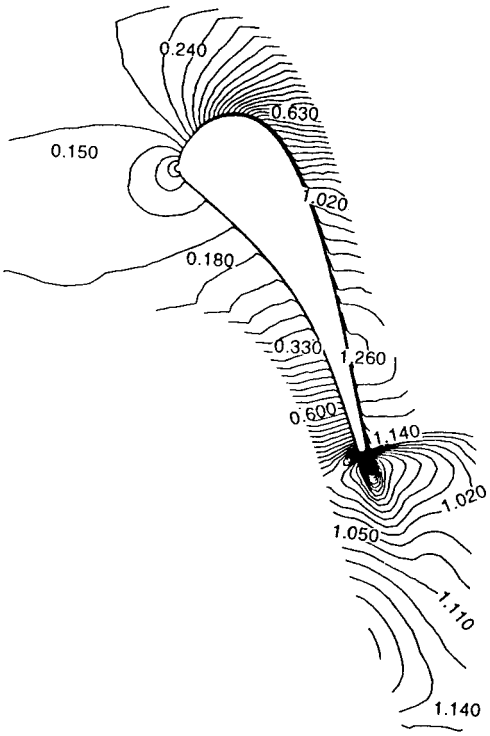

Fig. 4: Computed iso-Mach number contours for an isothermal wall uncooled VKI airfoil cascade.

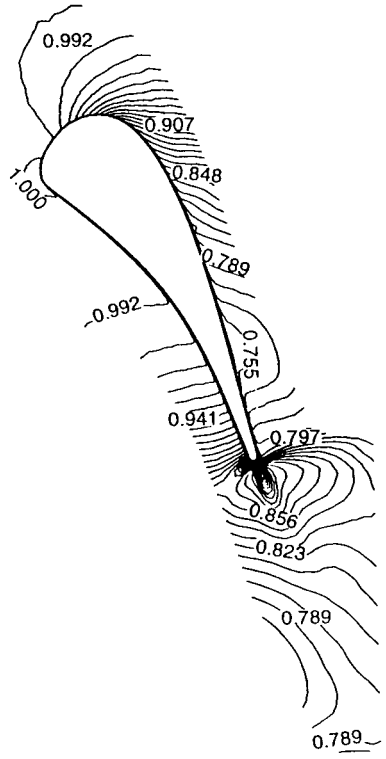

Fig. 5: Computed isotherms for an isothermal wall uncooled VKI airfoil cascade.

coefficient, h, distribution along the airfoil surface against the experimental data is shown in Fig. 6. The predicted pattern of heat transfer matches the experimental data reasonably well, but the actual predicted values in the leading edge region and on the pressure side are lower than in the experimental data. This shift is likely caused by the turbulence and transition models used. They appear to need further research in order to make them suitable for high turbulence heat transfer problems, as already noted in the VKI reports (Arts *et al.* 1990, page 13). Another likely cause of this shift is the non-smoothness of the geometric data provided in the VKI report. Consequently, these geometric data need to be smoothed with higher order splines (Larsson, 1997).

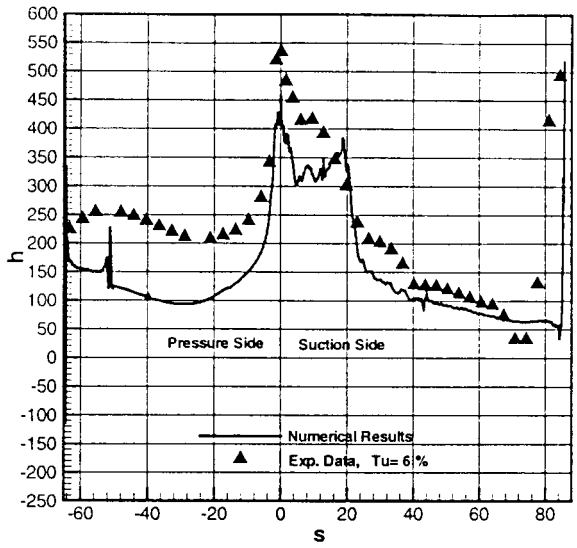

Fig. 6: Heat transfer coefficient distribution along an isothermal wall uncooled VKI airfoil cascade surface contour.

The next test case was the conjugate heat transfer prediction for a 1-D transonic turbulent flow around an internally coded axial turbine airfoil cascade with four internal coolant passages (Fig. 7). This configuration was generated by our own geometry generator for internally cooled axial turbine blades since we were not able to find any publicly available geometrical and experimental data for such configurations. The hybrid triangular/quadrilateral grid in the fluid region (Fig. 8) was composed of

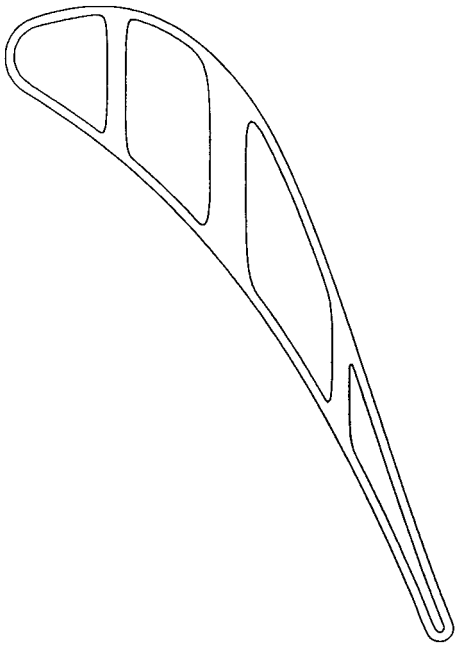

Fig. 7: Cascade airfoil with four internal coolant passages.

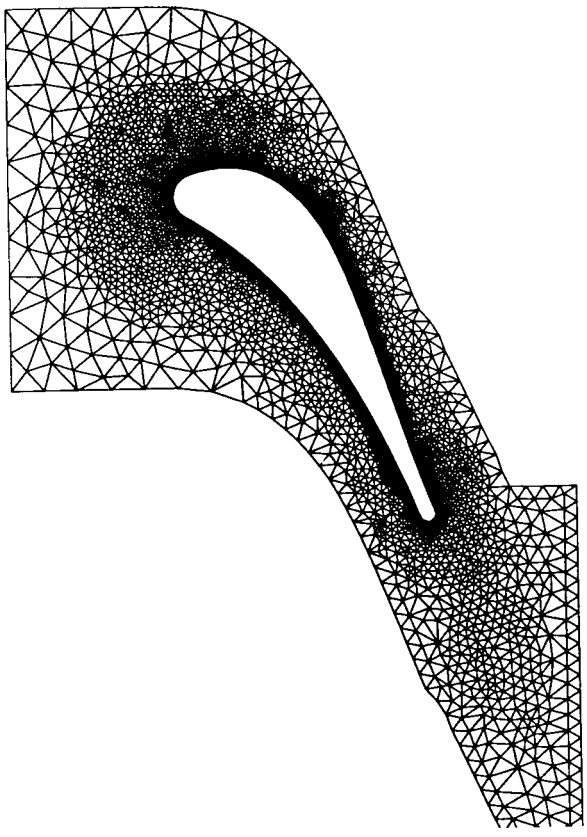

Fig. 8: Triangular-quadrilateral hybrid grid for the cascade airfoil flow-field.

seven structured O-grid layers (2208 quadrilaterals) which were used to resolve the boundary layer flow in the vicinity of the airfoil surface and 6496 triangles (3493 points) in the outer flow region. Inside the solid material the grid consisted of 3242 triangular elements. Figure 9 shows the combined grids in the leading edge region. The cascade operated under the following conditions: inlet total temperature of 1651.0 K, inlet total pressure of 597312.1 Pa, and average exit static pressure of 225740.0 Pa.

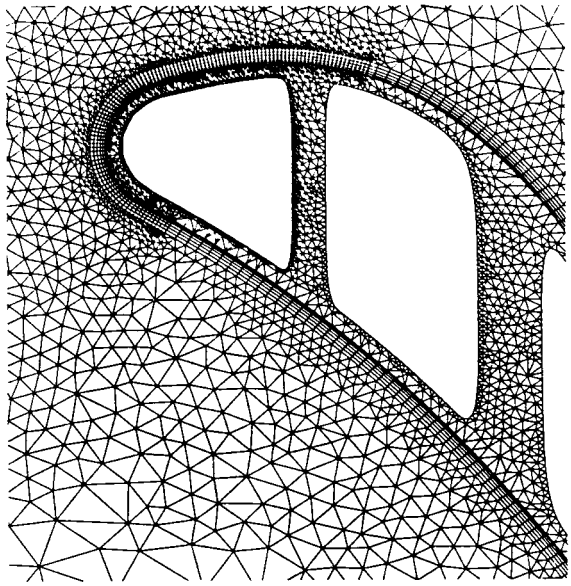

Fig. 9: Conjugate grids in the leading edge region of the cascade airfoil.

As stated originally, the objective of this conjugate heat transfer prediction algorithm is to automatically predict both temperature and heat flux distributions on the hot surface of the airfoil. This still leaves the user with the difficult task of having to specify thermal boundary conditions on the coolant passage walls, since these boundary conditions strongly depend on the coolant flow-field conditions in the passages. In the present work, we used an approximate method to specify thermal boundary conditions there. Given the coolant core flow bulk temperature, T_c, and the coolant wall average convective heat transfer coefficient, h, the

local heat flux q_w on the coolant passage wall is

$$q_w = -h(T_c - T_w)/\kappa \qquad (3)$$

Here, κ is thermal conductivity of the blade material, and T_w is the coolant passage wall non-uniform temperature which was iteratively updated during the conjugate heat transfer computations. Because the coolant bulk temperature, T_c, and the convective heat transfer coefficient, h, may be roughly predicted by empirical methods, it is realistic to specify heat flux on the coolant walls with equation (3) without solving the coolant flow-field. In our test case, we used T_c = 900.0 K, h = 2000 W m^{-2} K^{-1} and κ = 25.0 m^{-1} K^{-1}.

The computed iso-Mach number contours are presented in Fig. 10. The maximum Mach number in the flow-field is 1.653 and there is a strong shock-boundary layer interaction on the suction surface causing flow separation and an asymmetric pair of

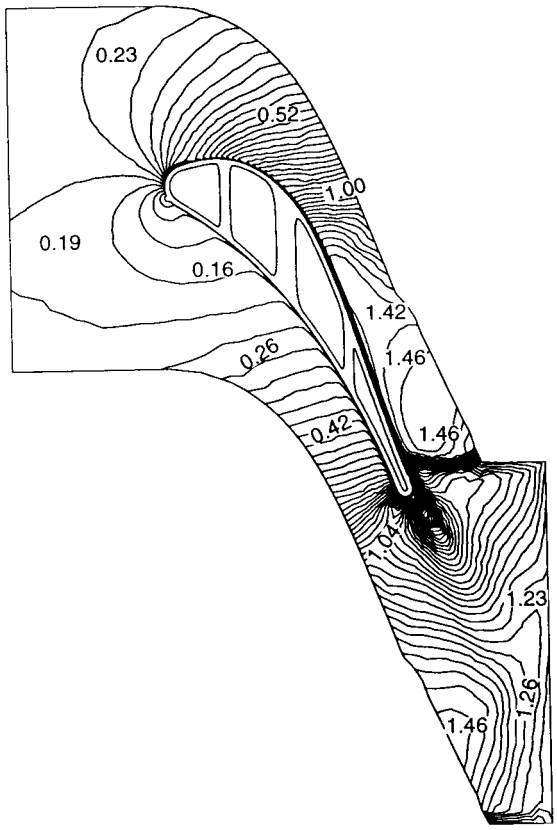

Fig. 10: Computed iso-Mach contours for a 2-D VKI cascade airfoil.

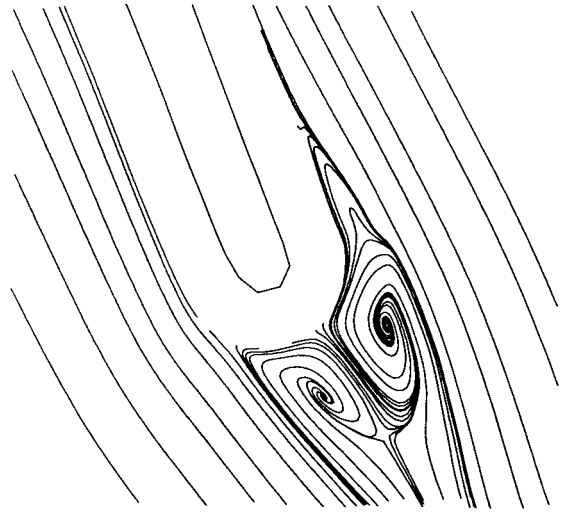

Fig. 11: Computed stream lines in the trailing edge region of a 2-D internally cooled cascade airfoil.

vortices attached to the trailing edge (Fig. 11).

The computed isotherms were non-dimensionalized by the inlet total temperature. These isotherms are depicted in the entire computational region (Fig. 12), the near leading edge region (Fig. 13), and in the trailing edge region (Fig. 14). At the leading edge, predicted material temperature was about 82% of the inlet total temperature. At the trailing edge, it was 76% of the inlet total temperature. This difference is due to the large amount of heat removed from the flow-field. The predicted temperature distributions on the blade surface and coolant passages (Fig. 15) are fully compatible with both the hot gas flow-field, the temperature field in the blade material, and the specified coolant bulk temperature and coolant passage wall heat transfer coefficients.

Three-Dimensional Validation

The 3-D heat transfer simulation code was first validated for the case of a pure heat conduction in a hollow sphere. The unstructured grid discretizing this domain had 104,544 tetrahedrons. Isothermal boundary conditions were specified on both inner and outer spherical surfaces as 1.0 and 0.25 respectively. A comparison of analytical and computed

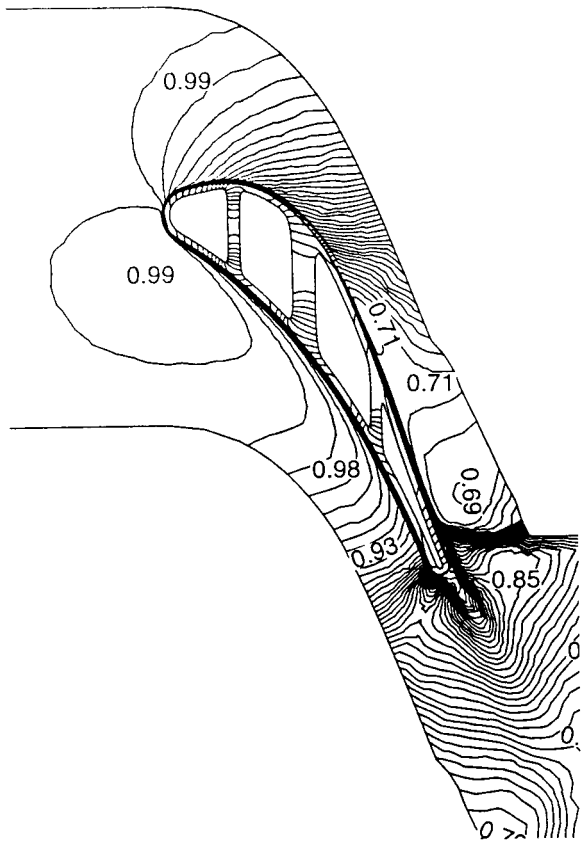

Fig. 12: Conjugate isotherms computed for a 2-D internally cooled cascade airfoil.

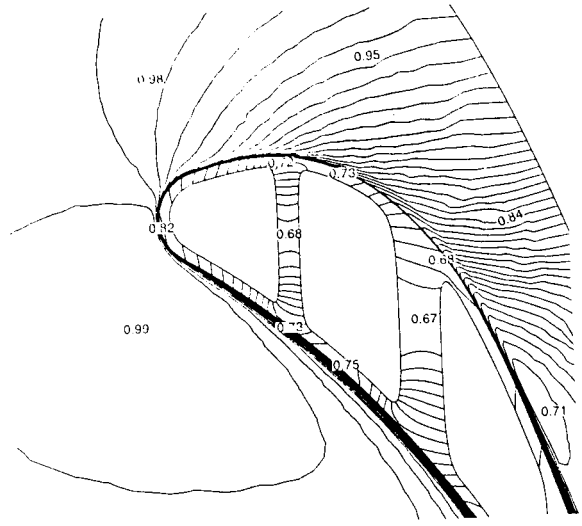

Fig. 13: Conjugate isotherms computed in the leading edge region of a 2-D internally cooled cascade airfoil.

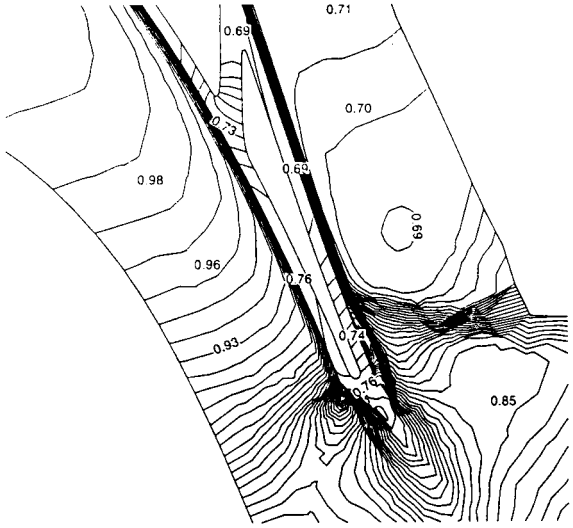

Fig. 14: Conjugate isotherms computed in the trailing edge region of a 2-D internally cooled cascade airfoil.

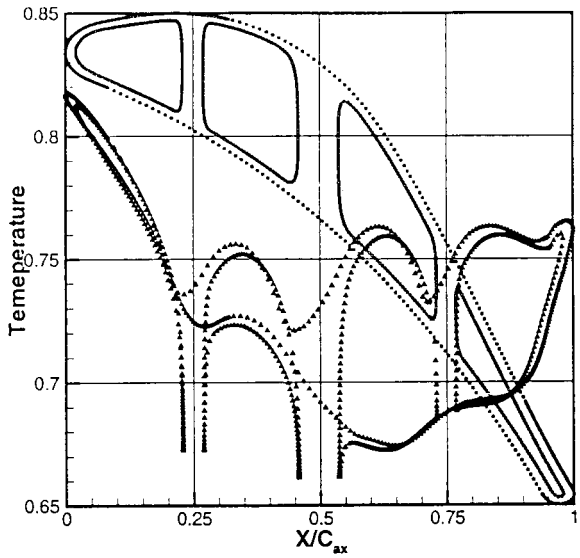

Fig. 15: Temperature distributions computed on the external and internal surfaces of a 2-D internally cooled cascade airfoil.

temperature distributions in the radial direction (Fig. 16) confirms the accuracy of the 3-D heat conduction analysis code.

Due to the lack of availability of hybrid unstructured grid generation tools for 3-D arbitrarily shaped turbine blades with internal coolant flow passages,

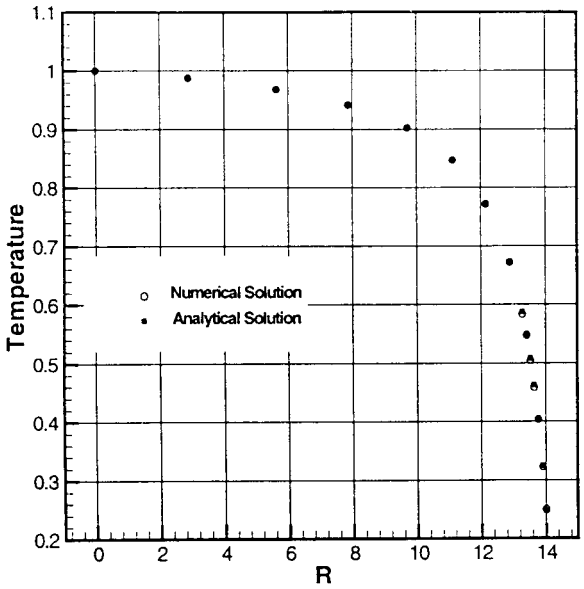

Fig. 16: Radial temperature distribution in a hollow sphere with isothermal surfaces.

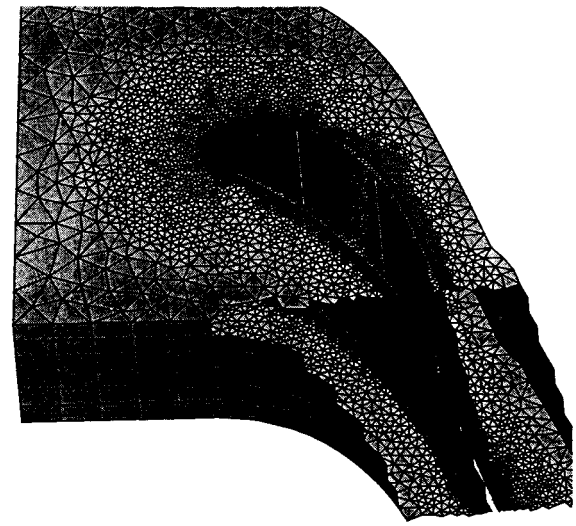

Fig. 17: Flow-field/heat transfer conjugate 3-D non-structured hybrid grid (z-clip).

our 2-D triangular grid generation code and structured quadrilateral grid generation code were used to generate hybrid unstructured 3-D grid around each airfoil and inside the airfoil with coolant holes. The 2-D triangular/quadrilateral hybrid grids outside an airfoil are depicted in Fig. 8. The 2-D hybrid grids outside and inside the airfoil were combined (as shown in Fig. 9) and stacked in spanwise direction with seven sections to form a 3-D aero-thermo conjugate computational prismatic grid of the turbine blade (Fig. 17). This prismatic/hexahedral grid is applicable only to straight planar turbine blades.

The airfoil of the straight internally cooled turbine blade and its flow conditions were the same as in the case of the 2-D internally cooled cascade. The objective was to test the accuracy of the 3-D conjugate heat transfer analysis code that utilizes a hybrid non-structured grid. The 3-D blade geometry used slip boundary conditions specified on the flat hub and flat shroud surfaces, thus creating flow-field conditions that are identical to those in a 2-D cascade. The thermal boundary conditions on the coolant passage walls were specified in the same way as in the 2-D case, that is, heat flux q_w was given by equation (3). The values for h, κ, and T_c were set to be the same in all regions and equal to the values used in the 2-D case.

Figures 18 – 21 show the results of the aero/

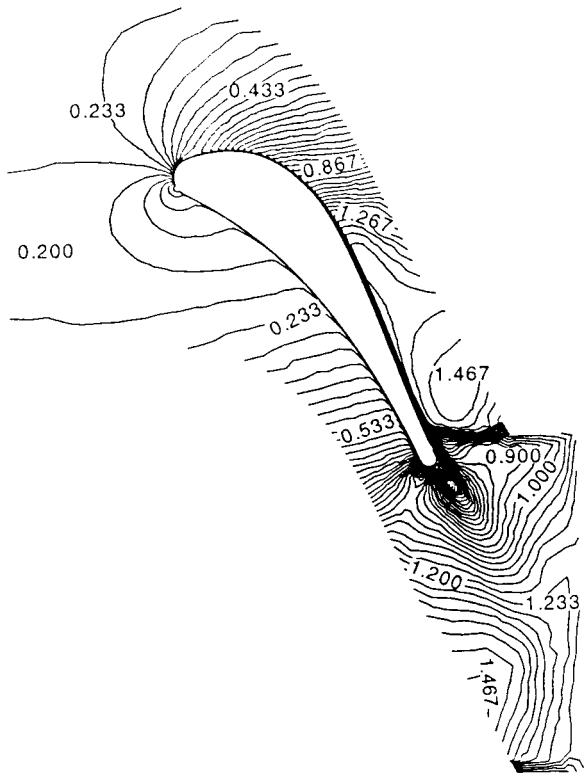

Fig. 18: Iso-Mach number contours computed with the 3-D conjugate analysis code.

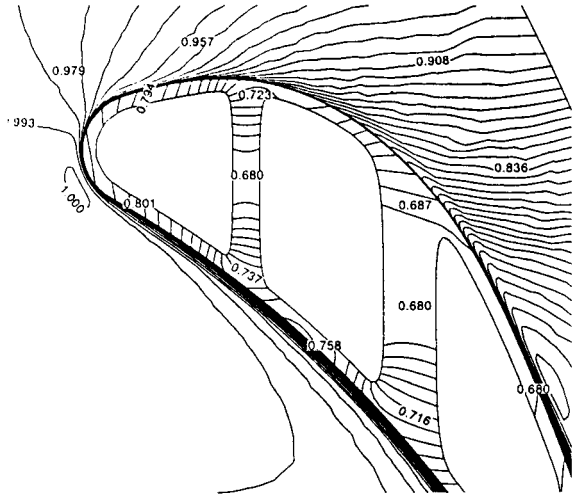

Fig. 19: Conjugate isotherms computed in the leading edge region of a 3-D internally cooled blade.

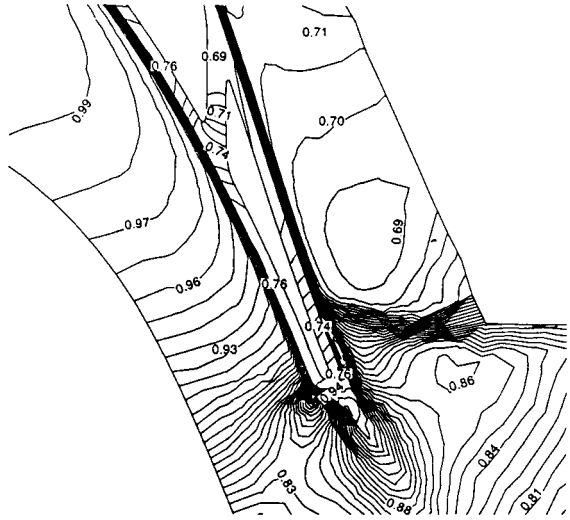

Fig. 20: Conjugate isotherms computed in the trailing edge region of a 3-D internally cooled blade.

thermo conjugate computation on the mid-span surface of the straight planar turbine blade. Figure 18 shows computed iso-Mach number contours around the blade. Comparison with the 2-D result (Fig. 10) indicates that, because of the slip boundary conditions on the flat shroud and hub surfaces, the 3-D and the 2-D computations result in an effec-

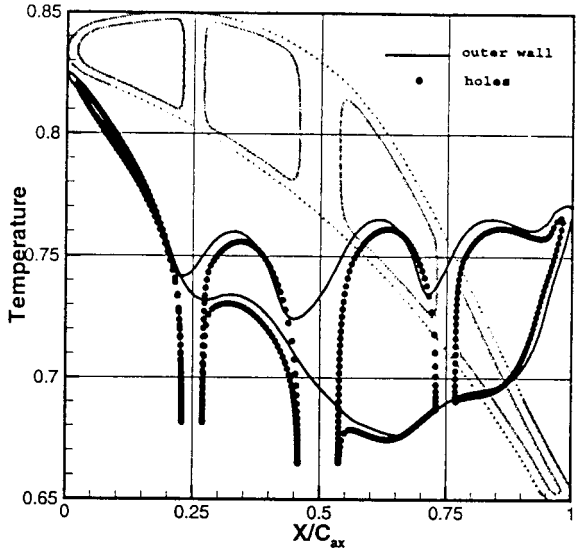

Fig. 21: Temperature distributions computed on the external and internal surfaces of a 3-D internally cooled blade.

tively identical flow-field. The predicted isotherms in the leading edge (Fig. 19) and the trailing edge (Fig. 20) regions compare very well with the corresponding 2-D calculations (Fig. 13 and Fig. 14). The minimum non-dimensional temperature predicted inside the blade is about 0.68 (in the middle of the second strut) and the maximum is 0.822 (in the leading edge),while the coolant core temperature is 0.454. The non-dimensional temperature predicted in the trailing edge region inside the blade is around 0.77. In the supersonic expansion region aft of the throat of this blade cascade the maximum Mach number is about 1.56 and the non-dimensional temperature is about 0.681.

The computed temperature distributions on the blade hot surface and the coolant passage surfaces are shown in Fig. 21. The temperature on the blade pressure side is higher than on its suction side. In a region before trailing edge temperature on the suction side is higher than on the pressure side (see also Figs. 19 and 20) and both of them are increasing, possibly due to flow separation and transition. The temperatures on the suction surface and on the pressure surface become closer at the strut locations and form necks there. This phenomenon is expected because of the high heat conductivity of

the struts, which connect the pressure side with suction side of the blade.

Conclusions

We have developed both 2-D and 3-D hybrid unstructured grid CFD analysis codes that can simultaneously predict the hot gas flow-field and the temperature field inside internally cooled configurations such as axial gas turbine blades. With this approach, temperatures and heat fluxes on the solid surfaces in contact with the moving fluid do not need to be specified since they are iteratively captured by the conjugate analysis code. These fully conjugate heat transfer prediction codes have been tested against analytical solutions for temperature fields due to steady heat conduction for simple geometries and experimental heat transfer results for uncooled airfoil cascades. The codes have also been successfully applied to realistically shaped 2-D internally cooled turbine airfoil cascades and 3-D internally cooled turbine blades. This general approach can be easily extended to include 3-D coolant flow-field computations, thus eliminating altogether the need for specification of thermal boundary conditions on external and internal blade surfaces.

Acknowledgements

The authors would like to express their gratitude for the National Science Foundation Grant DMKI-9522854 monitored by Dr. George A. Hazelrigg, the NASA Glenn Research Center Grant NAG3-1995 facilitated by Dr. John K. Lytle and monitored by Dr. Kestutis Civinskas, the Lockheed Martin Skunk Works grant monitored by Mr. Thomas Oatway, and the Penn State-Applied Research Laboratory grant monitored by Prof. Steven Garrett. The authors are also grateful for the experimental data provided by Dr. Paul Giel and Prof. J. Larsson.

References

T. Arts, M. Lambert de Rouvroit and A.W. Rutherford. "Aero-thermal investigation of a highly loaded transonic linear turbine guide vane cascade", VKI Technical Note 174, September, 1990.

D. Pelletier, L. Ignat and F. Ilinca. "An adaptive finite element method for conjugate heat transfer", AIAA Paper 95-0637, 1995.

J. Heidmann, D. Rigby and A. Ameri. "A three-dimensional coupled internal/external simulation of a film-cooled turbine vane", ASME Paper 99-GT-186, 1999.

D.E. Bohn, V.J. Becker, K.A. Kusterer, Y. Otsuki, T. Sugimoto and R. Tanaka. "3-D internal flow and conjugate calculations of convective cooled turbine blade with serpentine-shaped and ribbed channels", ASME Paper 99-GT-220, 1999.

R.V. Chima. "A k-ω turbulence model for quasi-three dimensional turbomachinery flows", AIAA Paper 96-0248 and NASA TM-107051, 1996.

N.T. Frink. "Recent progress toward a three-dimensional unstructured Navier-Stokes flow solver", AIAA Paper 94-0061, 1994.

P.W. Giel, D.R. Thurman, G.J. Van Fossen, S.A. Hippensteele and R.J. Boyle. "Endwall heat transfer measurements in a transonic turbine cascade", *ASME Journal of Turbomachinery*, **120**, 305-313 (1998).

P.W. Giel, G.J. Van Fossen, R.J. Boyle, D.R. Thurman and K.C. Civinskas. "Blade heat transfer measurements and predictions in a transonic turbine cascade", ASME Paper 99-GT-125, ASME International Gas Turbine Conference, Indianapolis, IN, 1999.

Z.-X. Han, R. Fang and Z.-J. Liu. "2-D flowfields calculation with multi-unstructured grids", *Journal of Aerospace Power*, **3**, 1999 [in Chinese].

A. Jameson and D. Mavriplis. "Finite volume solution of the two-dimensional Euler equations on a regular triangular mesh", *AIAA Journal*, **24** (4), 611-618 (1986).

J. Larsson. "Two-equation turbulence models for turbine blade heat transfer simulations", ISABE Paper 97-7163, 1997.

T.J. Martin, G.S. Dulikravich, Z.-X. Han and B.H. Dennis. "Minimizing coolant mass flow rate in internally cooled gas turbine blades", ASME Paper 99-GT-146, ASME Turbo Expo, Indianapolis, IN, June 7-10, 1999.

C.R. Mitchell. "Improved reconstruction scheme for the Navier-Stokes equations on unstructured meshes", AIAA Paper 94-0642, 1994.

P.L. Roe. "Characteristic based schemes for the Euler equations", *Annual Review of Fluid Mechanics*, **18**, 337-365 (1986).

J.M. Weiss and W.A. Smith. "Preconditioning applied to variable and constant density flows", *AIAA Journal*, **33** (11), 2050-2057 (1995).